Temperature dependence of the first-order Raman scattering by phonons in Si, Ge, and α-Sn: Anharmonic effects

José Menéndez and Manuel Cardona
Max-Planck-Institut für Festkörperforschung, Heisenbergstrasse 1, D-7000 Stuttgart 80, Federal Republic of Germany
(Received 23 June 1983; revised manuscript received 25 August 1983)

We have measured the temperature dependence of the first-order Raman scattering by phonons in Si, Ge, and α-Sn. The full widths at half maximum of the Raman lines, extrapolated to zero temperature, are 1.24 ± 0.07, 0.75 ± 0.03, and 0.81 ± 0.15 cm^{-1} for Si, Ge, and α-Sn, respectively. The reliability of the data obtained allows a critical examination of the theoretical calculations published so far. We show that the model assuming the decay of the Raman phonon into two acoustical phonons belonging to the same branch, first proposed by Klemens, does not represent adequately the temperature dependence of the Raman linewidth. The most important decay channels are shown to be combinations of optical and acoustical phonons. However, the more complete calculation by Cowley, which involves all possible decay channels, gives very large zero-temperature linewidths. We show that this arises mainly from the poor description of the phonon dispersion curves by the shell model used by Cowley, and that a better agreement between theory and experiment is to be expected by repeating the calculation with Weber's adiabatic bond-charge model.

I. INTRODUCTION

A large number of papers devoted to the study of the temperature dependence of first-order Raman scattering by phonons in semiconductors may be found in the literature.[1–9] However, considerable discrepancies between values for the linewidth reported by different authors, as well as theoretical calculations, still exist. In Table I we have selected some representative values for the full width at half maximum (FWHM) extrapolated to zero temperature for diamond and diamond-type semiconductors.

The reason for the experimental discrepancies displayed in Table I is often the finite resolution of the spectrometers. The corresponding corrections which have to be applied are sometimes as large as the width itself. On the other hand, no resolution corrections are needed to determine peak positions. Consequently, one finds rather good agreement between line shifts measured by different authors.

The question of the linewidths of tetrahedral semiconductors has recently gained renewed attention as a result of measurements of the lifetime τ of optical phonons in the time domain using laser-generated ultrashort pulses.[10,11] Preliminary measurements on GaAs (Ref. 11) seem to indicate that the lifetime is related to the frequency width through the energy-time uncertainty relation. This fact implies that the linewidth is determined by energy relaxation processes.

The linewidths of the optical $\vec{q}=0$ Raman phonons for diamond, silicon, and germanium have been calculated by Klemens[4] and Cowley.[5] Klemens's model is an attempt to keep the calculation in an analytically tractable form. To do this, the author assumes that the only contributions to the linewidth arise from terms which represent the decay of the Raman phonon into two acoustical phonons of op-

TABLE I. Some experimental and theoretical determinations of the FWHM of Raman phonons at zero temperature. The values corresponding to Klemens's theoretical model were calculated using Eqs. (12) and (27) of Ref. 4. Values given for Cowley's model correspond to calculations for 10 K.

Material		FWHM (cm^{-1})
Diamond	Krishnan[a] (expt.)	2.9
	Anastassakis *et al.*[b] (expt.)	2.0
	Borer *et al.*[c] (expt.)	1.68 ± 0.05
	Klemens[d] (theory)	0.035
	Cowley[e] (theory)	2.74
Silicon	Hart *et al.*[f] (expt.)	2.1
	Temple *et al.*[g] (expt.)	1.45 ± 0.05
	This work (expt.)	1.24 ± 0.07
	Klemens[d] (theory)	0.048
	Cowley[e] (theory)	11.34
Germanium	Ray *et al.*[h]	1.4
	Cerdeira *et al.*[i] (expt.)	1.1
	This work (expt.)	0.75 ± 0.03
	Klemens[d] (theory)	0.029
	Cowley[e] (theory)	5.34
α-Sn	This work (expt.)	0.81 ± 0.15
	Klemens[d] (theory)	0.047

[a]Reference 1.
[b]Reference 2.
[c]Reference 3.
[d]Reference 4.
[e]Reference 5.
[f]Reference 6.
[g]Reference 7.
[h]Reference 8.
[i]Reference 9.

posite $\vec{q}$ vector that belong to the same branch in the phonon dispersion curve. The matrix element is an *ad hoc* modification of matrix elements used in his theory of thermal conductivity. Although one can show by simple density-of-states arguments that Klemens's model is a gross oversimplification, it has gained wide acceptance, specially since the work of Hart *et al.*[6] on Si. The more complete calculation of Cowley,[5] summing over all possible decay processes and using a realistic anharmonic potential, surprisingly gives very large values for the linewidths of Si and Ge. Even the relative values of the widths with respect to diamond do not agree with the measurements.

Very recently, Balkanski *et al.*[12] repeated the linewidth measurements on Si, showing that Klemens's model does not fit the experimental data well. These authors modified the model by adding decay processes into three phonons of the same frequency.

We have performed measurements of Raman linewidths and line shifts for Si, Ge, and α-Sn as a function of temperature, using the same experimental setup and under conditions of high resolution. The reliability of the data obtained allows a critical examination of the theoretical models. Our measured linewidths cannot be satisfactorily explained with Klemens's model. We show that combinations of acoustical and optical phonons provide the most important decay channels for the $\vec{q}=\vec{0}$ optical Raman phonon in disagreement with the model of Ref. 12. The discrepancy of Cowley's calculation with our experimental values is shown to be mainly due to the inaccuracies in the shell-model description of the harmonic Hamiltonian. We estimate a semiquantitative correction that reduces the difference between theory and experiment to a factor of 2, a reasonable result in view of the simple anharmonic potential assumed in Cowley's model.

II. THEORY

A number of reviews dealing with the anharmonic shift and broadening of Raman lines have been published.[13–15] This work is based on an anharmonic contribution to the Hamiltonian, which can be written as[5]

$$H_A=\sum_{\vec{q}_1,\vec{q}_2,\vec{q}_3}\sum_{j_1,j_2,j_3} V\begin{bmatrix}\vec{q}_1 & \vec{q}_2 & \vec{q}_3\\ j_1 & j_2 & j_3\end{bmatrix} A(\vec{q}_1,j_1)A(\vec{q}_2,j_2)\vec{A}(q_3,j_3)$$
$$+\sum_{\vec{q}_1,\vec{q}_2,\vec{q}_3,\vec{q}_4}\sum_{j_1,j_2,j_3,j_4} V\begin{bmatrix}\vec{q}_1 & \vec{q}_2 & \vec{q}_3 & \vec{q}_4\\ j_1 & j_2 & j_3 & j_4\end{bmatrix} A(\vec{q}_1,j_1)A(\vec{q}_2,j_2)A(\vec{q}_3,j_3)A(\vec{q}_4,j_4)\,, \tag{1}$$

where

$$A(\vec{q},j)=a^{\dagger}_{-\vec{q},j}+a_{\vec{q},j}\,,$$

the a's being the usual phonon creation and annihilation operators.

The effect of these anharmonic interactions on the Raman-allowed optical mode is to change its harmonic frequency $\omega(\vec{0},j)$ to a damped frequency $\omega(\vec{0},j;\Omega)$ given by

$$\omega^2(\vec{0},j;\Omega)=\omega^2(\vec{0},j)+2\omega(\vec{0},j)[\Delta(\vec{0},j;\Omega)+i\Gamma(\vec{0},j;\Omega)]\,. \tag{2}$$

(The index j labels the three degenerate $\vec{q}=\vec{0}$ phonons.)

For the materials under consideration the real and imaginary parts of the self-energy, $\Delta(\vec{0},j;\Omega)$ and $\Gamma(\vec{0},j;\Omega)$ are much smaller than $\omega(\vec{0},j)$ and Eq. (2) can be rewritten as

$$\omega(\vec{0},j;\Omega)=\omega(\vec{0},j)+\Delta(\vec{0},j;\Omega)+i\Gamma(\vec{0},j;\Omega)\,. \tag{3}$$

Thus the line shape of the Stokes Raman peak becomes

$$I_s(\vec{0},j;\Omega)\propto\frac{\Gamma(\vec{0},j;\Omega)}{[\omega(\vec{0},j)+\Delta(\vec{0},j;\Omega)-\Omega]^2+\Gamma^2(\vec{0},j;\Omega)}\times[n(\Omega)+1]\,, \tag{4}$$

with the thermal occupation number

$$n(\Omega)=\frac{1}{\exp(\hbar\Omega/kT)-1}\,. \tag{5}$$

The function $\Delta(\vec{0},j;\Omega)$ gives the shift of the peak position. The three lowest-order contributions to the diagrammatic expansion of the self-energy yield[5]

$$\Delta(\vec{0},j;\Omega)=\Delta^{(0)}+\frac{12}{\hbar}\sum_{\vec{q},j'} V\begin{bmatrix}\vec{0} & \vec{0} & q & -q\\ j & j & j' & j'\end{bmatrix}[2n(\vec{q},j')+1]$$
$$-\frac{18\pi}{\hbar^2}\sum_{\vec{q},j_1,j_2}\left|V\begin{bmatrix}\vec{0} & \vec{q} & -\vec{q}\\ j & j_1 & j_2\end{bmatrix}\right|^2[n(\vec{q},j_1)+n(-\vec{q},j_2)+1]\left[\frac{1}{\omega(\vec{q},j_1)+(\vec{q},j_2)-\Omega}\right]_P\,, \tag{6}$$

with $n(\vec{q},j)=n(\omega(\vec{q},j))$ given in Eq. (5).

The first term in Eq. (6) is the thermal-expansion contribution to the line shift. It may be written[3] as

$$\Delta^{(0)}=\omega(\vec{0},j)\exp\left[-3\gamma(\vec{0},j)\int_0^T\alpha(T')dT'\right], \tag{7}$$

where $\alpha(T)$ is the coefficient of linear thermal expansion and $\gamma(\vec{0},j)$ is the Grüneisen parameter for the optical Raman mode. This term, as well as the fourth-order contribution to $\Delta(\vec{0},j;\Omega)$ [the second term in Eq. (6)], does not depend on Ω.

The broadening of the Raman line is given by

$$\Gamma(\vec{0},j;\Omega)=\frac{18\pi}{\hbar^2}\sum_{\vec{q},j_1,j_2}\left|V\begin{bmatrix}\vec{0} & \vec{q} & -\vec{q}\\ j & j_1 & j_2\end{bmatrix}\right|^2[n(\vec{q},j_1)+n(-\vec{q},j_2)+1]\delta(\omega(\vec{q},j_1)+\omega(-\vec{q},j_2)-\Omega)\,. \tag{8}$$

The last terms in Eqs. (6) and (8) are the third-order contributions to the shift and width, respectively. They are related by a Hilbert transform (dispersion or Kramers-Kronig relation).[16] The physical meaning of Eq. (8) is quite transparent: Owing to the anharmonic interactions the optical Raman phonon decays in a combination of two phonons $\omega(\vec{q},j_1)$ and $\omega(-\vec{q},j_2)$ satisfying $\omega(\vec{q},j_1)+\omega(-\vec{q},j_2)=\Omega$. We shall omit from now on the index $\vec{0},j$ in $\omega(\vec{0},j)$, $\Delta(\vec{0},j;\Omega)$, and $\Gamma(\vec{0},j;\Omega)$ since, for the materials under consideration, we are only concerned with one set of threefold-degenerate phonons at $\vec{q}\simeq\vec{0}$. Hence we define $\omega_0\equiv\omega(\vec{0},j)$, $\Delta(\Omega)\equiv\Delta(\vec{0},j;\Omega)$, and $\Gamma(\Omega)\equiv\Gamma(\vec{0},j;\Omega)$.

If the matrix elements in Eq. (8) are assumed to be constant, one obtains, for $\Gamma(\Omega)$, a value proportional to the two-phonon density of states when $T\to 0$,

$$\Gamma(\Omega)\propto\frac{1}{V}\sum_{\vec{q},j_1,j_2}\delta(\omega(\vec{q},j_1)+\omega(-\vec{q},j_2)-\Omega)\equiv\rho^2(\Omega)\,. \tag{9}$$

Equation (9) implies that one should expect a large $\Gamma(\Omega)$ whenever the frequency ω_0 of the optical mode happens to coincide with a peak in the two-phonon density of states. The matrix elements which determine the width $\Gamma(\Omega)$ are actually given by

$$V\begin{bmatrix}\vec{0} & \vec{q} & -\vec{q}\\ j & j_1 & j_2\end{bmatrix}=\frac{1}{6}\left[\frac{\hbar^3}{8NM^3\omega_0\omega(q,j_1)\omega(-q,j_2)}\right]^{1/2}\times\sum_{l',l''}\sum_{k,k',k''}\sum_{\alpha,\beta,\gamma}\phi_{\alpha\beta\gamma}\begin{bmatrix}0 & l' & l''\\ k & k' & k''\end{bmatrix}e_\alpha(k\mid\vec{0},j)e_\beta(k'\mid\vec{q},j_1)e_\gamma(k''\mid-\vec{q},j_2)e^{i\vec{q}\cdot[\vec{R}(l')-\vec{R}(l'')]}\,, \tag{10}$$

where

$$\phi_{\alpha\beta\gamma}\begin{bmatrix}0 & l' & l''\\ k & k' & k''\end{bmatrix}$$

is the third derivative of the interatomic potential with respect to displacements along directions of the Cartesian coordinates α, β, and γ of the atoms

$$\begin{bmatrix}0\\ k\end{bmatrix},\quad\begin{bmatrix}l'\\ k'\end{bmatrix},\quad\begin{bmatrix}l''\\ k''\end{bmatrix},$$

respectively. The index l labels the primitive cells, while k labels the position of the two atoms within the primitive cell. The vectors $\vec{e}(k\mid\vec{q},j)$ are the eigenvectors of the harmonic problem. M is the atomic mass and N the number of cells in the crystal.

It has been shown[17] that the phonon dispersion curves for diamond, silicon, germanium, and grey tin may be approximately scaled if one plots the relative frequency ω/ω_p as a function of qa, where ω_p is the ion plasma frequency ($\omega_p\sim M^{-1/2}a^{-3/2}$) and a is the lattice constant (this scaling is a good approximation for Si, Ge, and α-Sn, but not as good for diamond). Thus if one writes a scaled potential as

$$\phi(\ldots,\vec{u}_{lk},\ldots,\vec{u}_{l'k'},\ldots)=Ma^2\omega_p^2\Phi\left[\ldots,\frac{\vec{u}_{lk}}{a},\ldots,\frac{\vec{u}_{l'k'}}{a},\ldots\right], \tag{11}$$

where Φ is the same function for all materials, and replaces it in Eqs. (10) and (8), one finds

$$\Gamma(\Omega)\propto 1/Ma^2\,. \tag{12}$$

In Table II we compare Eq. (12) with the experimental linewidths extrapolated to zero temperature.

Two evaluations of Eq. (8) have been reported. Klemens[4] assumes that the optical Raman phonon decays in two acoustical phonons of opposite $\vec{q}$ belonging to the same branch. This means $j_1=j_2$ in Eq. (8) (there is *a priori* no reason for making this approximation. The density of states for combinations of two phonons with $j_1\neq j_2$ is actually much larger than that corresponding to $j_1=j_2$ as may be seen in Table III). The assumption $j_1=j_2$ leads to $\omega(\vec{q},j_1)=\omega(-\vec{q},j_2)$ and one obtains a broadening of the form

TABLE II. Comparison of the measured Raman FWHM $2\Gamma'(0)$ for $T\rightarrow 0$ with the prediction of the scaling theory [Eq. (12)]. The constant C has been chosen so as to normalize $C2\Gamma'(0)Ma^2$ to 1 for silicon.

	Diamond	Si	Ge	α-Sn
$\frac{1}{Ma^2}$(cgs)	3.94×10^{37}	7.27×10^{36}	2.58×10^{36}	1.21×10^{36}
$2\Gamma'(0)$ (cm^{-1})	1.68[a]	1.24[b]	0.75[b]	0.81[b]
$CMa^2[2\Gamma'(0)]$	0.25	1.0	1.7	3.9

[a]Reference 3.
[b]This work.

$$\Gamma(\omega_0,T)=\Gamma(\omega_0,0)[1+2n(\omega_0/2)]\ . \tag{13}$$

The constant $\Gamma(\omega_0,0)$ is determined by making further approximations to compute the matrix elements and the density of states. The values calculated with Klemens's model are listed in Table I. They are much smaller than the experimental linewidths. Our measurements show that even considering $\Gamma(\omega_0,0)$ to be an adjustable parameter, as is usually done,[2,6] the temperature dependence of Eq. (13) does not fit well the data. This indicates that processes with $j_1\neq j_2$ do contribute signficantly to the linewidth.

Cowley[5] made the first full calculation of Eq. (8) and the last term of Eq. (6). He solved the harmonic problem with a shell model[18,19] and assumed the anharmonic contribution to be an axially symmetric force between nearest neighbors. This anharmonic interaction has two parameters which were obtained by calculating the thermal expansion and fitting it to experimental results. The calculated $\Gamma(\omega_0)$ for diamond is in reasonable agreement with experiment, but the Γ's obtained for Si and Ge are larger than the experimental ones by a factor of the order of 10. We shall show that this discrepancy arises mainly from the poor description of the phonon dispersion curves by the shell model.

III. EXPERIMENT

The experiments were performed in the usual backscattering configuration. A Kr^+ laser was used as the exciting light source. The scattered light was analyzed with a Jarrell-Ash 1-m double monochromator and detected by photon counting. The data were transferred to a Digital Equipment Corporation PDP-11/34 computer and fitted with the appropriate line shape (usually a Lorentzian; see below).

The silicon sample we measured was a (100)-oriented high-purity wafer ($\rho>10^3$ Ω cm) provided by Wacker Chemitronic GmbH. The germanium sample was intrinsic at room tempeature, and oriented in the (111) direction. The α-Sn sample was a 500-Å-thick film grown on a (100)-oriented InSb surface using the molecular-beam-epitaxy technique of Farrow *et al.*[20] Photoemission experiments on these samples have already been reported.[21]

The low-temperature part of the measurements was performed in a Leybold helium cryostat and the high-temperature data were obtained by placing the sample in a glass oven whose pressure was kept below 10^{-5} Torr. The temperature was measured with a platinum resistor, and checked with existing data for the line shift. In order to avoid sample heating effects we have chosen a cylindrical lens to focus the incoming beam on the sample. The laser power was kept below 100 mW. No changes in the spectra were observed when reducing the applied power by a factor of 2.

Owing to the high-absorption coefficient of α-Sn in the visible and near ir ($\alpha=5\times10^5$ cm^{-1} for $\hbar\omega=1.92$ eV),[22] the Raman measurements on this material are particularly difficult. We have chosen to work with the 7525-Å laser line as near as possible to the E_1 maximum of the Raman efficiency.[23]

Silicon has a strong Raman signal and was measured with the same 7525-Å line. The Ge sample was measured with the 6471-Å line, which is closer to the E_1 gap resonance.

To achieve high resolution one has to reduce the slit widths in the spectrometer and increase the integration times. For the low-temperature data of α-Sn we needed typically 1 h/10 cm^{-1}. The measured phonons are so narrow that even with the reduced slits one has to correct for the finite instrumental resolution. The observed peak is the convolution of the Lorentzian shape of the actual phonons with the response function of the spectrometer. This function should have a triangular shape, but is very often considered to be a Gaussian. For the experiments under consideration, results obtained by assuming either triangular or Gaussian response functions are almost identical (within 3%). We have used Gaussian shapes for the actual calculations reported here.

The convolution product of a Gaussian times a Lorentzian curve is the so-called Voigt profile.[24] The rigorous procedure to make the deconvolution would be to

TABLE III. Two-phonon combined density of states $\rho^2(\Omega)$ for $\Omega=\Omega_0$, the Raman phonon frequency extrapolated to zero temperature. Values were determined by normalizing the curves of Go (Ref. 33) which give the two-phonon density of states calculated within Weber's adiabatic bond-charge model (Ref. 17). $\rho^2(\Omega_0)$ in units of $(a^3\omega_0)^{-1}$.

Material	Overtones ($j_1=j_2$)	Combinations ($j_1\neq j_2$)
Diamond	13	19
Silicon	4	50
Germanium	5	54

fit a Voigt profile to our experimental peaks, and then to calculate the Lorentzian linewidth using the fitted width of the Voigt profile and the experimentally determined width of the spectrometer response function. However, for a typical Raman experiment one needs a signal-to-noise ratio better than 100 to distinguish between the Voigt profile relevant to this work and Lorentzian curves with the same FWHM.[3] Our signal-to-noise ratio is about 25 (and worse for α-Sn), and therefore we used a simplified procedure.

The experimental peaks were fitted with a Lorentzian function, and the FWHM so obtained was assumed to be equal to the FWHM that one would find by fitting the experimental peaks with a Voigt profile. Then we corrected for the finite resolution of the spectrometer by using Posener's tables.[24] The width of the response function of the spectrometer was determined by measuring the linewidth of the laser line with the same slit apertures as in the Raman experiment.

The corrected linewidth obtained after the deconvolution procedure cannot be immediately related to the function $\Gamma(\Omega)\equiv\Gamma(\vec{0},j;\Omega)$ in Eq. (8). The reason is the Ω dependence of $\Delta(\Omega)$ and $\Gamma(\Omega)$ in Eq. (4) (Ref. 25) [$n(\Omega)$ is a very slowly varying factor]. The solution Ω_m of the equation

$$\Omega_m=\omega_0+\Delta(\Omega_m) \tag{14}$$

is conventionally regarded[26] as the position of the center of the Raman peak. If we now expand $\Delta(\Omega)$ in the neighborhood of Ω_m

$$\Delta(\Omega)=\Delta(\Omega_m)+\Delta_1(\Omega-\Omega_m)\,, \tag{15}$$

with

$$\Delta_1=\left.\frac{d\Delta(\Omega)}{d\Omega}\right|_{\Omega=\Omega_m}, \tag{16}$$

then Eq. (4), in the vicinity of Ω_m, can be written as

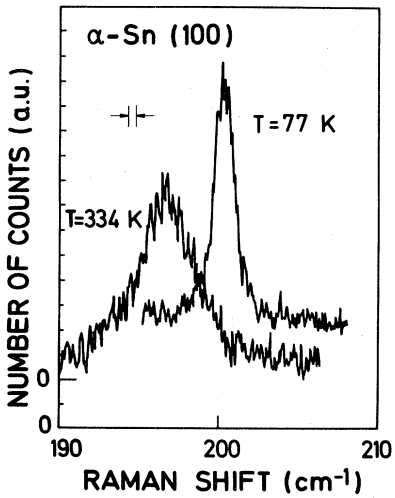

FIG. 1. Two typical Raman spectra for α-Sn at different temperatures.

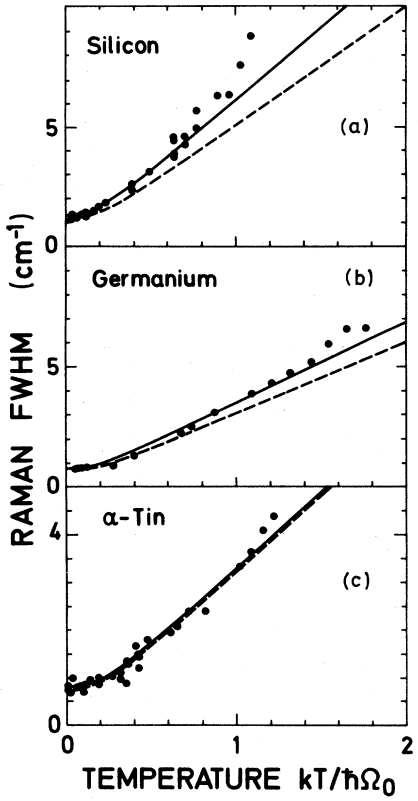

FIG. 2. Measured FWHM of the Raman peak as a function of the normalized temperature $kT/\hbar\Omega_0$ (points). Resolution correction discussed in Sec. III has been applied. Solid line is a fit with Eqs. (19a) and (19c). Dotted line is the prediction of Klemens's model [Eqs. (19a) and (19b)] setting $2\Gamma(0)$ equal to the experimental linewidth extrapolated to zero temperature. Ω_0 is the Raman frequency for $T\to 0$.

$$I_s(\Omega)=\frac{1}{1-\Delta_1}\,\frac{\Gamma'(\Omega_m)}{(\Omega-\Omega_m)^2+\Gamma'^2(\Omega_m)}[n(\Omega_m)+1]\,. \tag{17}$$

The half width at half maximum (HWHM) of the Lorentzian function of Eq. (17) is given by

$$\Gamma'(\Omega_m)=\frac{\Gamma(\Omega_m)}{1-\Delta_1}\,. \tag{18}$$

The Lorentz width obtained with the deconvolution procedure is $\Gamma'(\Omega_m)$ and not $\Gamma(\Omega_m)$, the value calculated in Eq. (8). Both widths are related by Eq. (18). In other words, to compare experimental and theoretical linewidths one needs, in principle, a calculation of both real and imaginary part of the self-energy.

IV. RESULTS

Two typical spectra for α-Sn are shown in Fig. 1. The spectra of Si and Ge look similar except for a better signal-to-noise ratio. Note that the peak of grey tin still appears at 334 K well above the transition temperature for the $\alpha\leftrightarrow\beta$ transformation of bulk tin [$\sim$286 K (Ref. 20)]. This demonstrates the stabilizing influence of the substrate. A detailed account of this phenomenon will be published elsewhere.

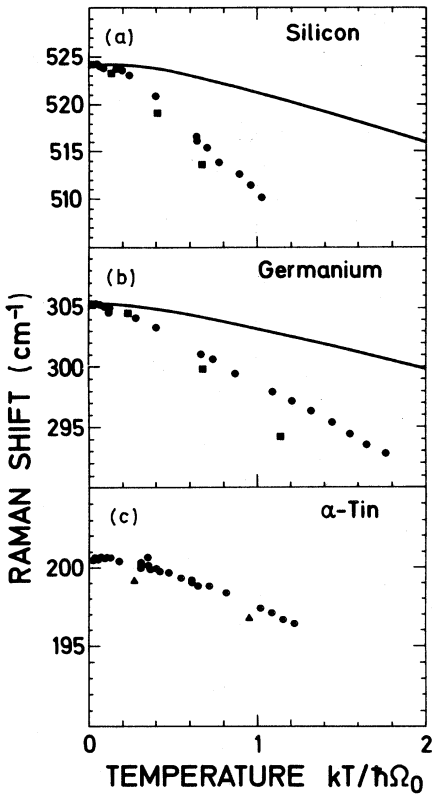

FIG. 3. Raman shift as a function of the normalized temperature $kT/\hbar\Omega_0$ (points). Solid line in Figs. 3(a) and 3(b) is the thermal-expansion contribution to the line shift. Squares represent Cowley's calculation plus the effect of thermal expansion. Triangles indicate the Raman shift obtained for bulk α-Sn samples (Ref. 29).

Figures 2(a)—2(c) show the measured linewidths versus temperature and Figs. 3(a)—3(c) the corresponding line shifts. The resolution correction applied amounts to 10% in Si and Ge and 30% for α-Sn at low temperatures ($T\sim 4$K). The measured linewidths for Si are much smaller than those reported by Hart *et al.*[6] Our room-temperature value, $2\Gamma'(300\text{ K})\sim 2.5\text{ cm}^{-1}$, agrees fairly well with measurements using a five-pass Fabry-Perot spectrometer, $2\Gamma'(300\text{ K})\sim 2.7\pm 0.1\text{ cm}^{-1}$.[27]

In Figs. 3(a)—3(c) we plot the shift in the Raman frequency versus temperature. The solid line in Figs. 3(a) and 3(b) represents the thermal-expansion contribution to the line shift, after Eq. (9), using $\gamma_{\text{Si}}(\vec{0},j)=0.98$, $\Gamma_{\text{Ge}}(\vec{0},j)=1.13$, and the integral $\int_0^T \alpha(T')dT'$ tabulated in Ref. 28. The results of Cowley's calculations are also represented (squares), whereby we have added the shift due to the thermal expansion to that calculated in Ref. 5. The calculated results were shifted so as to bring them into agreement with the measurements at low temperatures.

In Fig. 3(c) we indicate two values for the Raman shift obtained in bulk samples (triangles).[29] We notice that the Raman frequencies of the films are higher than the bulk ones by about 0.8 cm^{-1}. This shift can be attributed to the compression of the film due to the mismatch of the lattice parameters of α-Sn and InSb. The distorted lattice parameter of the film has been measured by Farrow *et al.*[20] Using the values of Ref. 20 and the anharmonicity parameters of Bell[30] for InSb (there are no data for α-Sn), we calculate for a film oriented along (100) a shift of 0.6 cm^{-1}, in reasonable agreement with the observation above.

V. DISCUSSION

We emphasize again that the experimentally measured linewidths (Fig. 2) are the $\Gamma'(\Omega_m)$ of Eq. (18) and not the imaginary parts of the phonon self-energy $\Gamma(\Omega_m)$. To compute the corresponding corrections one needs the spectral dependence of $\Delta(\Omega)$ calculated at each temperature. At some frequencies Δ_1 is of the order of 1 and the correction is large. For Ge we estimate at point Y of Fig. 4, which, as will be seen below, corresponds to the frequency $\Omega_m=\Omega_0$, $\Delta_1=-0.03$ at $T=10$ K, and $\Delta_1=-0.13$ at $T=300$ K. Hence corrections for the linewidth may become important at high temperatures. $\Gamma(\Omega_m)$ should be somewhat larger than $\Gamma'(\Omega_m)$. Unfortunately, we cannot perform them because no systematic calculation of $\Delta(\Omega)$ as a function of temperature is available in the literature. In the remainder of this section we discuss the three theoretical approaches which can be used to interpret the data of Figs. 2 and 3.

A. Klemens's model

The correction of Eq. (18) is usually neglected, and the linewidths are fitted with functions of the form[2,3,6,12]

$$2\Gamma'(T)=2\Gamma(T)=2\Gamma(0)[1+n(\omega(\vec{q},j_1))+n(\omega(-\vec{q},j_2))]\,, \tag{19a}$$

with $\omega(\vec{q},j_1)+\omega(-\vec{q},j_2)=\Omega_0$, Ω_0 being the Raman phonon frequency extrapolated to zero temperature.

If the decay channels considered by Klemens are the most relevant ones, we should be able to fit the data with Eq. (19a) and the additional condition

$$\omega(\vec{q},j_1)=\omega(-\vec{q},j_2)=\Omega_0/2\,, \tag{19b}$$

which has the form of Eq. (13). This condition is only fulfilled for some acoustic branches with $j_1=j_2$.

In Fig. 2 we show the temperature dependence of $2\Gamma'(T)$ obtained with Eqs. (19a) and (19b) by taking $\Gamma(0)$ equal to the measured value of $\Gamma'(0)$ at low temperatures (dashed line). We note that for $\Delta_1<0$ and $|\Delta_1|$ increasing with temperature, as obtained from Fig. 4, the discrepancy found for Si and Ge between the predictions of Klemens's ansatz (19a) and (19b) and the experiment would become even larger, if one makes the correction of Eq. (18).

In Table III we show the values of the two-phonon density of states calculated at the Raman phonon frequency Ω_0. This table explains the poor agreement between Klemens's model and experiment. The number of decay channels with $\omega(\vec{q},j_1)\neq\omega(-\vec{q},j_2)$ (combinations) is much higher than the number of overtone decay channels ($j_1=j_2$), especially for Si and Ge. Klemens's model only considers overtone processes [Eq. (19b) with $j_1=j_2$], i.e., most of the possible decay channels are neglected. In gen-

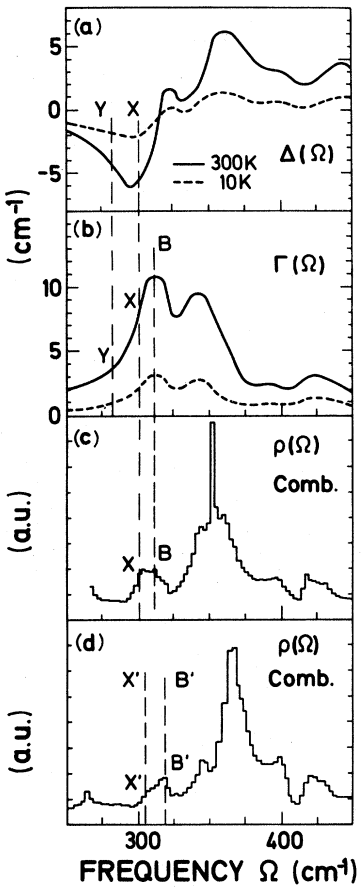

FIG. 4. Calculated self-energy (Ref. 5) and two-phonon combination density of states (Refs. 19 and 33) for Ge. (a) $\Delta(\Omega)$, dashed line: $T=10$ K; solid line: $T=300$ K. (b) $\Gamma(\Omega)$, dashed line: $T=10$ K; solid line: $T=300$ K. (c) Two-phonon density of states for combinations within the shell model used by Cowley (Ref. 19). (d) Same as (c), with Weber's adiabatic bond-charge model (Ref. 33). See text for explanation of X, Y, B, X', and B' lines.

eral, decay will take place into two phonons with $\omega(\vec{q},j_1)$ sweeping the range $0-\Omega_0$ and $\omega(\vec{q},j_2)=\Omega_0-\omega(q,j_1)$. Equation (19a) will be meaningful if the main contributions of the decay process cluster around one given frequency. An examination of the phonon dispersion relations suggests that this contribution arises from pairs (LA-LO) of phonons belonging to the Q branches[31] (along the $L-W$ line) and from nearby regions of the Brillouin zone. They fulfill the approximate relationship

$$\omega(\vec{q},j_1)=0.35\Omega_0,\quad \omega(-\vec{q},j_2)=0.65\Omega_0\ . \tag{19c}$$

A combined density-of-states calculation performed recently by means of a Brillouin-zone integration[32] shows indeed dominant peaks centered at the frequencies of Eq. (19c). We thus perform fits of the data of Fig. 2 with Eqs. (19a) and (19c) giving more weight to the low-temperature points so as to exclude decay processes into three or more phonons. Within the experimental temperature range the fit is rather good for α-Sn and for Ge. In the case of Si the fit is definitely better than with the assumption of Eq. (19b), although deviations at high temperatures may indicate either a breakdown of Eq. (19c) or increasing contribution of decay into three phonons, as suggested in Ref. 12. In the case of α-Sn the fits with Eqs. (19b) and (19c) have the same quality. Because of the analogy with Ge and Si, however, we believe the situation of Eq. (19c) to prevail also in this case.

B. Cowley's anharmonic lattice-dynamical calculations

As shown in Table I these calculations yield too large values for the phonon linewidths. This is surprising in view of the fact that Cowley's approach is more realistic than Klemens's. The reason can be found, at least in part, by analyzing Fig. 4. We shall concentrate our analysis on Ge because Cowley[5] only published the full calculated curve of $\Delta(\Omega)$ and $\Gamma(\Omega)$ for this material. However, we expect the analysis to be valid also for Si due to the very similar shape of the two-phonon density of states.[33] No calculations of phonon self-energies are available for α-Sn.

Figure 4(c) represents the density of combination ($j_1\neq j_2$) states calculated with the shell model by Cowley.[19] Figure 4(d) gives the same density of states obtained from Weber's model.[33] One sees that in the latter the structure near Ω_0 is shifted towards higher energies. This is exactly what one would find by looking at experimental dispersion curves: Weber's model provides a much better fit to them. The density of states $\rho(\Omega_0)$ (X' line) is now lower than in Cowley's shell model. On the other hand, the matrix elements should also be smaller: If one compares Figs. 4(b) and 4(c) in the region between 275 and 325 cm^{-1}, it follows that the matrix elements tend to increase towards higher energies. Therefore, the fact that in Weber's model all features are shifted towards higher energies leads to a lower $\rho(\Omega)$ and to a smaller matrix element at $\Omega=\Omega_0$. We have made an attempt to evaluate this semiquantitatively in the following way: As may be seen in Figs. 3(a) and 3(b), the calculated line shifts are somewhat larger than the experimental ones. Let us consider in Fig. 4 the line X, which represents the Raman phonon frequency in Cowley's calculation. If we move this towards the left, in order to equate the experimental and theoretical shifts, we obtain the line Y. The value of the width is reduced by a factor of 2.6, and the difference between experimental and theoretical linewidths reduces to a factor of 2. In making this correction we are neglecting the fourth-order contribution to the line shift. There are some indications that this term is smaller than the thermal-expansion shift. For example, the line shift of diamond is almost entirely due to a thermal-expansion effect.[2,3] The difference between the experimental points and the thermal-expansion term is just the third-order contribution to the line-shift calculated by Cowley (see Fig. 3 of Ref. 3), so that the fourth-order term must be small over a large temperature range.

A difference of a factor of 2 between theory and experiment, as estimated above, would not be a surprise because there are some indications that Cowley's anharmonic potential is not completely adequate. The mode-Grüneisen parameters,[18] for example, do not agree well with experiment and with those calculated by Yin and Cohen.[34] A

new calculation of $\Gamma(\Omega)$ with Weber's model would permit us to establish to what extent the potential assumed by Cowley has to be modified.

C. Scaling approach

In Table II we compare the predictions of Eq. (12) with the experimental linewidths. If the four elements would follow a scaling law, all values in the third line of Table II would be 1. We thus conclude that either the density of states or the matrix elements or both do not scale as assumed. Small deviations from the scaling law for the dispersion relations can lead to large variations in the density of states *near critical points.* Table III exhibits clearly the difference between diamond and the semiconducting elements: The relative density of *combination* states is much smaller in diamond than in Si and Ge. The reason for this is the flattening of TA phonons away from the zone center for the latter materials, i.e., a deviation from the scaling law. If we assume that the matrix elements for combinations and overtones are not very different, we can explain the very low relative value of the linewidth for diamond as partly due to the small density of combination states.

The relatively large half width of gray tin can also be understood in the following way: As we see from Fig. 4 (this figure refers to Ge, but the corresponding curves for Si and α-Sn must be rather similar, as discussed above), the frequency of the Raman phonon, indicated by the X line, happens to be near a peak in the density of two-phonon states. The X line indicates the position of ω_0 in Cowley's shell-model calculation ($\omega_0=300.5$ cm^{-1}) and the X' line indicates our experimental Raman frequency extrapolated to zero temperature ($\Omega_0=305.1$ cm^{-1}). In Weber's model the maximum of the peak in the density of states near Ω_0 (B' in Fig. 4) coincides with the combination of phonons belonging to the $Z_1(A)$ and Z_1 branches along the $X-W$ line.[17,33] If the frequency of this point is called $\omega_{B'}$ we estimate, from Refs. 17 and 32, that $\omega_{B'}/\Omega_0=1.05$, 1.05, and 0.97 for Si, Ge, and α-Sn, respectively. This means that for α-Sn, Ω_0 is closer to the peak in B' and to higher energies. Hence the Y line of Fig. 4 must be displaced to the right for this material. The result should be an increase in the linewidth with respect to Ge by about 50% which falls short of that given in Table II but at least represents the general trend.

VI. CONCLUSION

We have proved that the investigation of the temperature dependence of the first-order Raman scattering offers an important tool to check not only specific anharmonic properties, but also different models for the phonon dispersion curves in the harmonic approximation. Therefore, a full calculation of the phonon self-energy with Weber's model would be desirable in order to verify the correctness of the ideas discussed above concerning the inaccuracies of the shell model used by Cowley and their influence on the calculated linewidth.

From the experimental point of view, it would be interesting to study the Raman linewidth as a function of pressure. Owing to the difference in the mode-Grüneisen parameters, the Raman phonon is expected to shift with presssure towards higher frequencies faster than the two-phonon combinations that give rise to peak B's in Fig. 4(d). Referring to Cowley's calculation, the effect of pressure would be to shift line X towards line B, hence increasing the linewidth. This has not been observed in previous measurements,[35] probably due to poor experimental resolution.

ACKNOWLEDGMENTS

We gratefully acknowledge the technical assistance of H. Hirt, M. Siemers, and P. Wurster. We are indebted to H. Höchst and I. Hernández-Calderón for growing the α-Sn sample used in this experiment.

[1]R. S. Krishnan, Proc. Indian Acad. Sci. 24, 45 (1946).
[2]E. Anastassakis, H. C. Hwang, and C. H. Perry, Phys. Rev. B 4, 2493 (1971).
[3]W. J. Borer, S. S. Mitra, and K. V. Namjoshi, Solid State Commun. 9, 1377 (1971).
[4]P. G. Klemens, Phys. Rev. 148, 845 (1966).
[5]R. A. Cowley, J. Phys. (Paris) 26, 659 (1965).
[6]T. R. Hart, R. L. Aggarwal, and B. Lax, Phys. Rev. B 1, 638 (1970).
[7]P. A. Temple and C. E. Hathaway, Phys. Rev. B 7, 3685 (1973).
[8]R. K. Ray, R. L. Aggarwal, and B. Lax, in *Light Scattering in Solids,* edited by M. Balkanski (Flammarion, Paris, 1971), p. 288.
[9]F. Cerdeira and M. Cardona, Phys. Rev. B 5, 1440 (1972).
[10]J. Kuhl and W. E. Bron, in *Physics of Semiconductors,* edited by M. Averous (North-Holland, Amsterdam, 1983), p. 532.
[11]D. von der Linde, J. Kuhl and H. Klingenberger, Phys. Rev. Lett. 44, 1505 (1980).
[12]M. Balkanski, R. F. Wallis, and E. Haro, Phys. Rev. B 28, 1928 (1983).
[13]R. A. Cowley, Proc. Phys. Soc. London 84, 281 (1964).
[14]R. A. Cowley, Rep. Prog. Phys. 31, 123 (1968).
[15]E. R. Cowley and R. A. Cowley, Proc. R. Soc. London Ser. A 287, 259 (1965).
[16]A. A. Maradudin, A. E. Fein, and G. H. Vineyard, Phys. Status Solidi 2, 1479 (1962).
[17]W. Weber, Phys. Rev. B 15, 4789 (1977).
[18]G. Dolling and R. A. Cowley, Proc. Phys. Soc. London 88, 463 (1966).
[19]W. Kress, Diplomarbeit, University of Frankfurt am Main (1967).
[20]R. F. C. Farrow *et al.*, J. Cryst. Growth 54, 507 (1981).
[21]H. Höchst and I. Hernández-Calderón, Surf. Sci. 126, 25 (1983). See also Ann. Israel Phys. Soc. 6(I), 333 (1983).
[22]L. Viña (unpublished).
[23]M. Iliev, M. Sinyukov, and M. Cardona, Phys. Rev. B 16, 5350 (1977).

[24]D. W. Posener, Aust. J. Phys. 12, 184 (1959).
[25]We gratefully acknowledge Professor G. Strauch for bringing this point to our attention.
[26]I. P. Ipatova, A. A. Maradudin, and R. F. Wallis, Phys. Rev. 155, 882 (1967).
[27]M. Grimsditch and M. Cardona, Phys. Status Solidi B 102, 155 (1980).
[28]Y. S. Toulokian *et al.*, *Thermophysical Properties of Matter* (IFI-Plenum, New York, 1977), Vols. 12 and 13.
[29]C. J. Buchenauer, M. Cardona, and F. H. Pollak, Phys. Rev. B 3, 1243 (1971).
[30]M. I. Bell, Phys. Status Solidi B 53, 675 (1972).
[31]G. Nilsson and G. Nelin, Phys. Rev. B 3, 364 (1971).
[32]P. B. Allen (private communication).
[33]S. Go Sumargo, Ph.D. thesis, University of Stuttgart, 1975.
[34]M. T. Yin and M. L. Cohen, Phys. Rev. B 26, 3259 (1982).
[35]B. A. Weinstein and G. J. Piermarini, Phys. Rev. B 12, 1172 (1975).